

# Indication of the electron-to-proton mass ratio variation within the Galaxy

March 25, 2025

J. S. Vorotyntseva<sup>1</sup>, S. A. Levshakov

*Ioffe institute, Politechnicheskaya 26, St. Petersburg 194021 Russia*

## Abstract

Near ( $\approx 100$  pc) and far ( $\approx 8.7$  kpc) relative to the Galactic center, the molecular clouds SgrB2(N) and Orion-KL exhibit different values of the fundamental physical constant  $\mu = m_e/m_p$  – the electron-to-proton mass ratio. Measured frequency difference between the emission lines of methanol ( $\text{CH}_3\text{OH}$ ),  $-J_{K_u} \rightarrow J_{K_\ell} = 6_3 \rightarrow 5_2 A^+$  542000.981 MHz,  $6_3 \rightarrow 5_2 A^-$  542081.936 MHz, and  $8_0 \rightarrow 7_{-1} E$  543076.194 MHz, – observed with the space observatory *Herschel* toward SgrB2(N) and Orion-KL corresponds to (Sgr-Ori):  $\Delta\mu/\mu = (-3.7 \pm 0.5) \times 10^{-7}$  ( $1\sigma$  C.L.). At the same time, comparison of the same methanol lines in Orion-KL with laboratory frequencies shows no significant changes in  $\mu$  (Ori-lab):  $\Delta\mu/\mu = (-0.5 \pm 0.6) \times 10^{-7}$ , while a comparison between SgrB2(N) and laboratory lines indicates a lower value of  $\mu$  near the Galactic center (Sgr-lab):  $\Delta\mu/\mu = (-4.2 \pm 0.7) \times 10^{-7}$ . The reduced value of  $\mu$  in SgrB2(N) is not explained by known systematic effects and requires further investigation.

---

<sup>1</sup>j.s.vorotyntseva@mail.ioffe.ru

# 1 Introduction

Precision measurements of fundamental physical constants remain a long-standing challenge for both laboratory and space research. Under terrestrial conditions, experiments with atomic clocks, and, more recently, with nuclear clocks, have achieved extremely tight constraints on changes with time of dimensionless physical constant – the fine structure constant ( $\alpha = e^2/\hbar c$ ) at the level of  $10^{-19} \text{ yr}^{-1}$ , and the electron-to-proton mass ratio ( $\mu = m_e/m_p$ ) at the level of  $10^{-16} \text{ yr}^{-1}$ . Differential measurements of these quantities at different points of the Earth’s orbit under conditions of changing gravitational potential of the Sun also did not reveal appreciable deviations in the frequencies of the atomic clocks at the level of  $10^{-8}$ . Extensive material on this topic was collected by and analyzed in a recent review [1].

Spatial and temporal changes in physical constants are predicted in various theories extend the Standard Model of particle physics. The necessity for such extension arises, in particular, from attempts to explain the nature of dark matter. Since it has not been possible to detect dark matter particles so far, suggestions have been made about scalar fields that could manifest themselves as dark matter. These fields can modulate the masses of elementary particles, such as electrons and quarks, and, hence, should lead to small variations of  $\mu$  [2]-[6]. Changes of this kind can affect in turn the structure of energy levels in molecules, which can be detected experimentally.

The search for spatial and temporal variations in  $\mu$  is related to estimating the quantity

$$\Delta\mu/\mu = (\mu_{obs} - \mu_{lab})/\mu_{lab}, \quad (1)$$

where  $\mu_{lab}$  – the laboratory value of  $\mu$ , and  $\mu_{obs}$  – the value observed in the astronomical objects.

This comparison is possible due to the fact that the electro-vibro-rotational transitions in molecular spectra have a specific dependence on the local value of  $\mu$ , which is individual for each transition [7, 8]. The dependence on  $\mu$  is characterized by a dimensionless sensitivity coefficient,  $Q$ , which shows the reaction of a given molecular transition with a frequency  $f$  to a small change in  $\mu$ :

$$Q = \frac{df/f}{d\mu/\mu}, \quad (2)$$

where  $df/f$  is the relative frequency shift, and  $d\mu/\mu$  is determined by (1). The values of  $Q$  are calculated using quantum-mechanical methods for the

transition  $f = E_u - E_\ell$  using the so-called  $q$ -factor [9]:

$$\Delta f = q \frac{\Delta\mu}{\mu}, \quad (3)$$

where  $\Delta f$  is the frequency change caused by a small variation of  $\mu$ ,  $q = q_u - q_\ell$  (in  $\text{cm}^{-1}$ ), and

$$Q = \frac{q}{f}. \quad (4)$$

To estimate hypothetical variations of  $\mu$ , it is necessary to use pairs of lines with different sensitivity coefficients  $Q_1$  and  $Q_2$  observed in the same molecular cloud:

$$\frac{\Delta\mu}{\mu} = \frac{V_1 - V_2}{c(Q_2 - Q_1)}, \quad (5)$$

where  $V_1$  and  $V_2$  are the measured radial velocities, and  $c$  is the speed of light. Note that the conversion to the velocity scale from the frequency scale is carried out according to the radio astronomical convention

$$\frac{V}{c} = \frac{f_{lab} - f_{sky}}{f_{lab}}. \quad (6)$$

At present, the most stringent constraints on  $\mu$ -variations in the Galactic disk were obtained from observations of the inversion transition of ammonia  $\text{NH}_3$  ( $Q = 4.46$  [10]) and purely rotational transitions ( $Q=1$ )  $\text{HC}_3\text{N}$ ,  $\text{HC}_5\text{N}$  and  $\text{HC}_7\text{N}$ :  $\Delta\mu/\mu < 7 \times 10^{-9}$  [11]. Another perspective molecule for such purposes turned out to be methanol  $\text{CH}_3\text{OH}$ , and its isotopologues – methanol transitions have high sensitivity coefficients of both signs [9, 12, 13]. Constraints on  $\mu$ -variations based on observations of methanol in the Galaxy are established at the level of  $\Delta\mu/\mu < 1 \times 10^{-8}$  [14], and for extragalactic objects (at redshift  $z=0.89$ )  $\Delta\mu/\mu < 5 \times 10^{-8}$  [15].

Thus, the expected effect of hypothetical scalar fields on the masses of elementary particles was not revealed at this accuracy level.

## 2 Methods

The most significant problem in achieving a higher accuracy level ( $\sim 10^{-9}$ ) is the errors in laboratory frequencies, which are for methanol lines reach values of 50 kHz in the high frequency range ( $f \sim 540$  GHz). To reach the level of  $10^{-9}$ , the accuracy must be on the order of several kHz, which is

problematic in laboratory measurements. At the same time, astronomical observations make it possible to achieve a rather high accuracy acceptable for precision measurements of  $\Delta\mu/\mu$  at the level of  $10^{-9}$ .

To minimize the dependence on laboratory frequencies, a slightly modified approach can be used to estimate the  $\mu$ -variations, which is as follows. We offer to compare the difference of the measured frequencies ( $f_1 - f_2$ ) of the same pairs of methanol lines with different sensitivity coefficients  $Q_1$  and  $Q_2$  observed in two astronomical objects ( $a$ ) and ( $b$ ) at different galactocentric distances. It follows from the relations (1-4) that

$$\frac{\Delta\mu_{a,b}}{\mu} = \frac{\mu_a - \mu_b}{\mu_{lab}} = \frac{(f_{1,a} - f_{2,a}) - (f_{1,b} - f_{2,b})}{\Delta q}, \quad (7)$$

where  $f_{1,a}, f_{2,a}$  and  $f_{1,b}, f_{2,b}$  – the observed transition frequencies in the co-moving reference frame (corrected for the radial velocity  $V_{LSR}$  of the object), and  $\Delta q = q_1 - q_2$  – the difference of the  $q$ -factors of the compared lines. This method allows us to use only astronomical frequencies without resorting to laboratory measurements.

### 3 Observations and parameters of *Herschel* spectra

The spectra used in this work were taken from the archive of the space observatory *Herschel*<sup>2</sup> [16]. The observations were obtained using the instrument *HIFI* (Heterodyne Instrument for the Far-Infrared) with the Wide-Band Spectrometer *WBS* in *Spectral Scan* mode. This mode included observations with frequency tuning of the local oscillator (LO), which made it possible to obtain, after separating the lower (*LSB*) and upper (*USB*) frequency bands, a single spectrum of the object in a wide spectral range.

The technical characteristics of the observed range of 480–560 GHz (band 1a) are as follows: the telescope’s aperture at the center of the range is 40”, the width of the intermediate frequency band (IF) is 4 GHz, and the spectral resolution (channel width)  $\Delta_{ch} \sim 0.3$  km/s (500 kHz).

The median calibration error of the frequency scale for each of the four CCD arrays of *WBS* does not exceed 50 kHz with almost zero average shift of

---

<sup>2</sup>*Herschel* is an ESA space observatory with science instruments provided by European-led Principal Investigator consortia and with important participation from NASA.

Table 1: Object coordinates [16] and galactocentric distances  $D_{GC}$

Object	$R.A.$ (J2000)	$Dec.$ (J2000)	$D_{GC}$ , kpc
<b>Orion-KL</b>	$05^h35^m14.36^s$	$-05^\circ22'33.63''$	8.7
<b>SgrB2(N)</b>	$17^h47^m20.06^s$	$-28^\circ22'18.33''$	0.1

the center frequency of the spectral line for various LO frequencies in the test mode [17]. Also, no trends were detected within the intermediate frequency band in the CCD pixel-to-frequency transform.

From all the astronomical objects observed by the *Herschel*, we selected two – Orion-KL and SgrB2(N). Orion-KL is a large molecular gas complex in Orion, where star formation is actively taking place. SgrB2(N) is a massive molecular gas cloud in Sagittarius, located near the Galactic center, in which  $\Delta\mu/\mu$  estimates have never been performed before. The object coordinates – right ascension ( $R.A.$ ) and declination ( $Dec.$ ), as well as the distance from the Galactic center ( $D_{GC}$ ) are shown in Table 1.

We used high-level spectra (level 2.5) from the *Herschel* archive. The processing level 2.5 implies conversion to the scales of antenna temperatures  $T_A^*$  (in Kelvin) and observed frequencies  $f_{sky}$  (in GHz) [18]. The spectra for each astronomical object are provided in two polarizations – horizontal  $H$  and vertical  $V$ . We subtracted the continuum from each of these spectra and stacked them with weights inversely proportional to the squares of the noise levels.

## 4 Calculated line parameters

It is known from *Herschel* spectral surveys that microwave spectra of Orion-KL and SgrB2(N) [19, 20] have a rich molecular composition especially in the frequency band 480–560 GHz – from simple molecules (e.g., CO), to complex organic ones such as methanol ( $\text{CH}_3\text{OH}$ ). For our purposes, we selected three close methanol lines in the Orion-KL and SgrB2(N) spectra that fall in the same intermediate frequency band  $IF = 4$  GHz – two lines at 542 GHz and one at 543 GHz. This selection minimizes possible instrumental systematic errors, associated with *WBS* calibrations. The parameters of the selected methanol lines are presented in Table 2: transition, which can be described by two quantum numbers – the total angular momentum,  $J$ , and its projection onto the symmetry axis of the molecule,  $K$ , for the upper  $u$

Table 2: Parameters of the selected CH<sub>3</sub>OH transitions. Given in parentheses are the laboratory errors in the last digits.

Transition $J_{K_u} \rightarrow J_{K_\ell}$	$f_{lab}$ , MHz	$S\mu_e^2$ , $D^2$	$E_\ell$ , cm <sup>-1</sup>	$Q$
$6_3 \rightarrow 5_2A^+$	542000.981(50)	5.5658	50.413	0.0
$6_3 \rightarrow 5_2A^-$	542081.936(50)	5.5638	50.411	0.0
$8_0 \rightarrow 7_{-1}E$	543076.194(50)	4.1354	49.035	1.7

and lower  $\ell$  levels; the laboratory frequency  $f_{lab}$ ; the line strength  $S\mu_e^2$ ; the energy of the lower level  $E_\ell$  [21], and the sensitivity coefficient  $Q$  [22].

Table 2 shows that the molecular transitions have close energies of the lower levels, which means that they emit from the same region of the molecular cloud.

We used a multi-component Gaussian-like model to describe the line profile. At the same time, the minimum number of Gaussian components was decided, which provides  $\chi_\nu^2 \lesssim 1$ . The resulting envelope curves are shown in Fig. 1 in red color: left panel – the observed lines toward SgrB2(N), right panel – toward Orion-KL. For each line, the laboratory frequency, the noise level *rms*, the signal-to-noise ratio *SNR*, and the value of  $\chi_\nu^2$  are specified. The parameters of the observed lines are listed in Table 3 – the frequency at the envelope curve maximum  $f_{sky}$ , the corresponding radial velocity  $V_{LSR}$ , and the full width at half maximum line width *FWHM*.

Also, Table 3 lists the observed frequencies in the comoving reference frame  $f_c$  corrected for the average radial velocity  $V_{LSR}$ . It is determined along the lines  $6_3 - 5_2A^+$  and  $6_3 - 5_2A^-$ , which have zero sensitivity coefficients  $Q$ . For SgrB2(N), the average velocity  $\langle V_a \rangle = 65.12(2)$  km s<sup>-1</sup>, for Orion-KL –  $\langle V_b \rangle = 8.15(2)$  km s<sup>-1</sup>.

The last column in Table 3 gives an estimate of the expected accuracy of the line position. The expected statistical error of the center of a single Gaussian line profile is defined by the expression [23]

$$\sigma_f = 0.7 \frac{\Delta_{ch}}{SNR} \sqrt{FWHM/\Delta_{ch}}. \quad (8)$$

Table 3 shows that the analytical error estimates from (8) are almost identical to the numerical ones given in parentheses in the second column, which were obtained by the  $\Delta\chi^2$  method applied to the envelope curves.

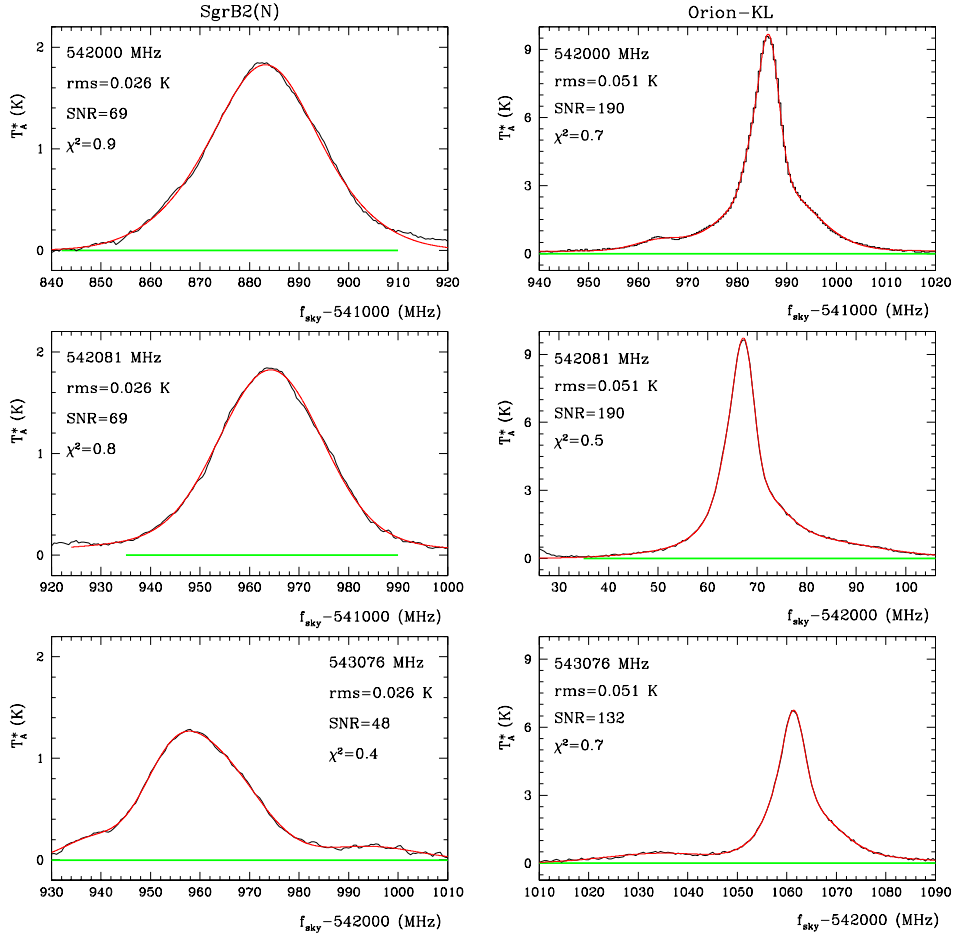


Figure 1: Methanol lines toward the two sources – SgrB2(N) and Orion-KL, obtained at the Herschel Space Observatory. The original spectra are shown in black, and the model spectra are shown in red. The horizontal green lines mark the ranges used in minimizing  $\chi^2$ . The line parameters are listed in Table 3.

Table 3: Parameters of the observed lines. The statistical errors in the last digits are shown in parentheses. ( $1\sigma$ ).

Object	$f_{sky}$ , MHz	$V_{LSR}$ , km s <sup>-1</sup>	$FWHM$ , MHz	$f_c$ , MHz	$\sigma_f$ , kHz
Orion-KL	541986.222(8)	8.16(3)	7.3	542000.964(8)	7
	542067.209(8)	8.15(3)	7.2	542081.953(8)	7
	543061.376(12)	8.18(3)	7.7	543076.147(12)	10
SgrB2(N)	541883.185(38)	65.16(4)	26.1	542000.921(38)	37
	541964.243(37)	65.09(3)	25.6	542081.996(37)	36
	542957.837(51)	65.34(4)	23.7	543075.806(51)	50

## 5 $\Delta\mu/\mu$ estimations and discussion

As noted above, to estimate the value of  $\Delta\mu_{a,b}/\mu$  two massive molecular clouds were chosen – SgrB2(N) (object *a*) and Orion-KL (object *b*). Estimates on  $\mu$ -variations are obtained from comparing the differences in the measured frequencies of methanol lines converted into the comoving reference frames of the *a* and *b* objects. Transitions with  $Q = 0$  at 542000 MHz and 542081 MHz, which were compared with the 543076 MHz transition having  $Q = 1.7$ , led to the following results:

$$\frac{\Delta\mu_{a,b}}{\mu} = (-3.2 \pm 0.7) \times 10^{-7} \quad (9)$$

for the 543076 and 542000 MHz lines, and

$$\frac{\Delta\mu_{a,b}}{\mu} = (-4.2 \pm 0.7) \times 10^{-7} \quad (10)$$

for the 543076 and 542081 MHz lines.

This provides the average value

$$\langle \Delta\mu_{a,b}/\mu \rangle = (-3.7 \pm 0.5) \times 10^{-7}. \quad (11)$$

The resulting error  $\sigma_{\Delta\mu/\mu}$  in this case is calculated as the square root of the sum of the squares of the measured frequency errors (see the fifth column in Table 3) divided by the difference of the  $q$ -factors  $\Delta q$  (this value is assumed to be known accurately). Errors in determining the average velocities  $\langle V_a \rangle$  and  $\langle V_b \rangle$  were not taken into account when converting the observed frequencies into comoving reference frames, since they are not dominant in the total error budget  $\sigma_{\Delta\mu/\mu}$ .

Another possible source of error is the calibration error  $\sigma_{\text{sys}} \lesssim 50$  kHz, discussed above. In our case, not absolute values of frequencies are compared, but their differences. Therefore the calibration error is leveled because the frequencies fall within the same band  $\text{IF} = 4$  GHz.

Thus, the result  $\langle \Delta\mu/\mu \rangle = (-3.7 \pm 0.5) \times 10^{-7}$  indicates the non-zero signal at  $7.5\sigma$ . Even if the frequency differences in these measurements are exposed to systematic shifts of  $\sim 50$  kHz, the statistical significance of the detected signal is not lost:  $\langle \Delta\mu_{a,b}/\mu \rangle = (-3.7 \pm 0.7) \times 10^{-7} (5.3\sigma)$ .

If we apply a different estimation method of  $\Delta\mu/\mu$  (equation (5)) separately to SgrB2(N) and to Orion-KL, the following mean values are obtained:

$$\langle \Delta\mu/\mu \rangle_a = (-4.2 \pm 0.7) \times 10^{-7}, \quad (12)$$



$$\langle \Delta\mu/\mu \rangle_b = (-5 \pm 6) \times 10^{-8}. \quad (13)$$

These results show that no signal is detected in Orion-KL, whereas SgrB2(N) exhibits a change in  $\mu$  at the confidence level of  $6\sigma$ .

We also note that the most stringent upper limits on  $\Delta\mu/\mu$  (see above) were obtained earlier from observations of molecular clouds in the Galactic disk located at relatively close distances to the Solar System,  $D_{GC} = 8.5 - 8.7$  kpc (galactocentric distance of the Solar System  $D_{GC} = 8.34$  kpc [24]). In this paper, we compare a relatively close object to the Solar System Orion-KL ( $D_{GC} = 8.7$  kpc), for which the signal at the level of  $10^{-8}$  is not detected, and SgrB2(N) in the center of the Galaxy, showing a lower ratio of  $\Delta\mu/\mu$ .

Since it is believed that the density ratio of baryonic matter,  $\rho_{BM}$ , to dark matter,  $\rho_{DM}$ , varies along the Galactic radius, and closer to the Galactic center  $\rho_{BM}/\rho_{DM} > 1$ , but at the periphery  $\rho_{BM}/\rho_{DM} < 1$ , it can be assumed that the detected signal in  $\Delta\mu/\mu$  correlates with the distribution of dark matter.

In conclusion, we summarize the main results of the work. A statistically significant variation of the fundamental physical constant  $\mu$  at the confidence level of  $7.5\sigma$  was found from a comparison of the same methanol lines ( $\text{CH}_3\text{OH}$ ) in two objects spaced approximately 9 kpc apart – SgrB2(N), located in the center of the Galaxy, and Orion-KL, located closer to the Galactic periphery. The measured relative shift of the spectral lines in methanol is not explained by known systematic effects, and can be interpreted as a manifestation of the interaction of dark matter with baryonic matter. However, to confirm this assumption, it is necessary to conduct independent measurements of  $\Delta\mu/\mu$  in other sources in the directions of the Galactic center and anticenter.

## Funding

This work was supported by ongoing institutional funding and was carried out within the framework of the topic of the State Assignment of the Ioffe Institute number FFUG-2024-0002. No additional grants to carry out or direct this particular research were obtained.

## Conflict of interest

The authors of this work declare that they have no conflicts of interest.

## References

- [1] J.-P. Uzan, Fundamental constants: from measurement to the universe, a window on gravitation and cosmology (2024) arXiv:2410.07281
- [2] R. Onofrio, Phys. Rev. D, **82**, 065008 (2010).
- [3] F.D. Albareti, A.L. Maroto, and F. Prada, Phys. Rev. D, **95**, 044030 (2017).
- [4] S. Alexander, J. D. Barrow, and J. Magueijo, CQG, **33**, 14LT01 (2016).
- [5] D. Antypas, A. Garcon, R. Ozeri, G. Perez et al. Phys.Rev.Lett. **123**, 14, 141102 (2019)
- [6] Y. V. Stadnik, V. V. Flambaum, Phys. Rev. Lett., **115**, 201301 (2015)
- [7] D.A. Varshalovich and S.A. Levshakov, JETP Lett. **58**, 237 (1993).
- [8] M.G. Kozlov and S.A. Levshakov, Ann. Phys., **525**, 452 (2013).
- [9] S.A. Levshakov, M.G. Kozlov, and D. Reimers, ApJ, **738**, 26 (2011).
- [10] V.V. Flambaum and M.G. Kozlov, Phys. Rev. Lett., **98**, 240801 (2007).
- [11] S.A. Levshakov, C. Henkel, D. Reimers, and P. Moralo, Mem. S. A. It., **85**, 90 (2014).
- [12] P. Jansen, L.H. Xu, I. Kleiner, W. Ubachs, and H.L. Bethlem, Phys. Rev. Lett., **106**, 100801 (2011).
- [13] J.S. Vorotyntseva, M.G. Kozlov, and S.A. Levshakov, MNRAS, **527**, 2750 (2024).
- [14] Vorotyntseva J.S., Levshakov S.A., JETP Letters, **119**, 9, 649 (2024)
- [15] N. Kanekar, W. Ubachs, K. M. Menten, J. Bagdonaite, A. Brunthaler, C. Henkel, S. Muller, H. L. Bethlem, M. Dapra, MNRAS, **488**, L104 (2015)
- [16] <https://archives.esac.esa.int/hsa/whsa/>

- [17] I. M. Avruch, Cycle38 Frequency Calibration Tests, Tech. Rep. HIFI-ICC-TN-2015-002, SRON Groningen (2011)
- [18] D. Teyssier, I. Avruch, S. Beaulieu, J. Braine, A. Marston, P. Morris, M. Olberg, M. Rengel, R. Shipman, The Heterodyne Instrument For The Far Infrared (HIFI) Handbook, HERSCHEL-HSC-DOC-2097, version 2.1, 157 pp. (2017)
- [19] N. R. Crockett, E. A. Bergin, J. L. Neill, C. Favre, G. A. Blake, E. Herbst, D. E. Anderson and G. E. Hassel, *ApJ*, **806**, 239 (2015)
- [20] J. L. Neill, E. A. Bergin, D. C. Lis, P. Schilke, N. R. Crockett, C. Favre, M. Emprechtinger, C. Comito, S.-L. Qin, D. E. Anderson, A. M. Burkhardt, J.-H. Chen, B. J. Harris, S. D. Lord, B. A. McGuire et al., *ApJ*, **789**, 8 (2014)
- [21] L.-H. Xu and Lovas F.J., *J. Phys. Chem. Ref. Data*, **26**, 1 (1997)
- [22] P. Jansen, L.-H. Xu, I. Kleiner, W. Ubachs, and H. L. Bethlem, *Phys. Rev. Lett.* **106**, 100801 (2011), Suppl. material
- [23] D.A. Landman, R. Roussel-Dupre and G. Tanigawa, *ApJ* **261**, 732 (1982)
- [24] P. Mege, D. Russeil, A. Zavagno, D. Elia, S. Molinari, C. M. Brunt, R. Butora, L. Cambresy, A. M. Di Giorgio, T. Fenouillet, Y. Fukui, J. C. Lambert, Z. Makai, M. Merello, J. C. Meunier et al., *A&A*, **646**, A74 (2021)